



Biphenotypic Sinonasal Sarcoma with a Novel *PAX3::FOXO6* Fusion: A Case Report and Review of the Literature

Meredith M. Nichols¹ · Fatimah Alruwaili¹ · Mohamad Chaaban² · Yu-Wei Cheng³ · Christopher C. Griffith¹

Received: 1 July 2022 / Accepted: 17 July 2022 / Published online: 28 September 2022
© The Author(s), under exclusive licence to Springer Science+Business Media, LLC, part of Springer Nature 2022

Abstract

Background Biphenotypic sinonasal sarcoma (BSS) is a low-grade, locally aggressive sarcoma unique to the sinonasal region. BSS is most common in middle aged patients and affects women more frequently than men. It is characterized by a bland spindled cell proliferation with neural and myogenic differentiation. BSS are usually associated with rearrangement t(2;4)(q35;q31.1) resulting in a *PAX3::MAML3* fusion. Less commonly, other genes are found in combination with *PAX3* and some cases reported in the literature have an unknown fusion partner.

Methods A 54-year-old man presented with nasal mass. Endoscopic resection showed a low-grade spindle cell neoplasm with morphologic features of BSS and immunohistochemical and next generation sequencing were performed to confirm the diagnosis.

Results The tumor was positive for S100 and smooth muscle actin but negative for SOX10. Next generation sequencing demonstrated a novel *PAX3::FOXO6* gene fusion.

Conclusions Although a *PAX3::FOXO6* gene fusion has never been reported, this finding combined with the morphologic and immunophenotypic features supports the diagnosis of BSS.

Keywords Biphenotypic sinonasal sarcoma · *PAX3:FOXO6* · TRK

Introduction

Biphenotypic sinonasal sarcoma (BSS) is a low-grade, locally aggressive sarcoma that arises exclusively in the sinonasal region. There is a considerable female predominance (~2:1) and the peak incidence is in the 5th decade.[1, 2] BSS show both neural and myogenic differentiation and were originally described as “low-grade sinonasal sarcoma with neural and myogenic features.”[3] This pattern of differentiation can be confirmed by immunohistochemistry

with positive expression of S100 and smooth muscle actin in most cases.[4] BSS is classically associated with the recurrent t(2;4)(q35;q31.1) gene rearrangement resulting in a *PAX3::MAML3* gene fusion.[5] *PAX3* over-expression by IHC has also been shown to be a useful in distinguishing BSS from morphologic mimickers.[6] Subsequent studies have also demonstrated other chromosomal rearrangements in BSS, mostly with *PAX3* and alternative fusion partners including some with unidentified partner genes. Here, we describe a case of BSS with a *PAX3::FOXO6*, a novel fusion that has previously not been described in BSS or any other tumor to our knowledge.

✉ Christopher C. Griffith
griffic8@ccf.org

¹ Department of Anatomic Pathology, Robert J. Tomsich Pathology & Laboratory Medicine Institute, Cleveland Clinic, Cleveland, OH, USA

² Department of Otolaryngology, Section of Nasal and Sinus Disorders, Head and Neck Institute, Cleveland Clinic, Cleveland, OH, USA

³ Department of Laboratory Medicine, Robert J. Tomsich Pathology & Laboratory Medicine Institute, Cleveland Clinic, Cleveland, OH, USA

Case Report

A 54-year-old man with a past medical history of sarcoidosis and remote nasal injury initially presented with persistent headaches. Over several weeks, he developed postnasal drip, thickened nasal secretions, and epistaxis after sneezing. These symptoms were also associated with an inability to breathe through the right side of his nose. He was

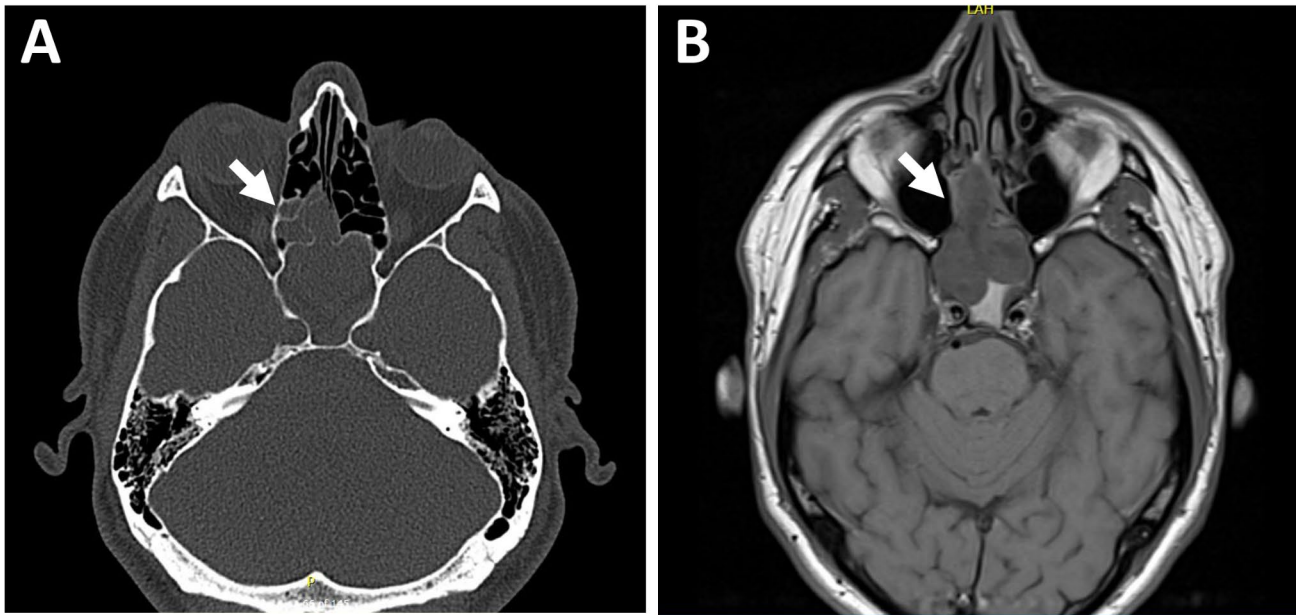


Fig. 1 Pre-operative imaging findings. **A** CT without contrast demonstrated a mucosal mass adherent to the right middle turbinate (arrow). **B** MRI with contrast showed the mass extended into the sphenoid sinus with involvement of the right posterior ethmoid air cells, possibly compatible with an inverted sinonasal papilloma (arrow)

subsequently referred to otolaryngology. Nasal endoscopy was performed and showed bilateral posterior nasal polyps. He was started on corticosteroids with mild improvement in breathing.

Computed tomography of the sinuses showed a mucosal polyp adherent to the posterior right middle turbinate. Remodeling of the inferior portion of the posterior right ethmoid labyrinth and opacification of the posterior right ethmoid air cells with complete opacification of the right sphenoid sinus chamber were noted (Fig. 1 A and 1B). The sphenoid sinus appeared effaced. Magnetic resonance imaging (MRI) of the face showed a polypoid sinonasal mass that measured 4.9 cm in greatest dimension with extension into the sphenoid sinus and involved the right posterior ethmoid air cells (Fig. 1 C). There was no evidence of osseous erosion in the imaging studies. Radiographically, these findings raised the possibility of an inverted sinonasal papilloma.

Due to the patient's symptoms and imaging findings, he underwent endoscopic removal of the mass. A frozen section was performed on the right nasal mass and showed a polypoid lesion with atypical stromal cells. The right nasal mass and sphenoid sinus contents were subsequently resected

piecemeal, along with separately submitted extended mucosal margins.

Pathologic findings

Histologic examination showed a submucosal spindle cell neoplasm with variably myxoid to collagenous background (Fig. 2 A). The tumor had an alternating pattern of cellular fascicles with intervening lobular myxoid hypocellular areas. In the more conventional cellular areas the tumor had fascicular and herringbone arrangement of cells in a collagenous background (Fig. 2B C). In contrast, lobular hypocellular areas with more prominent myxoid stroma showed a sharp demarcation from more cellular areas (Fig. 2D) giving a low power appearance reminiscent to that usually seen in myxofibrosarcoma. Infiltrative growth was evident microscopically with entrapment of submucosal glands and pre-existing bony trabeculae (Fig. 2E). Despite the variable cellularity, the neoplastic cells appeared uniform throughout the lesion with eosinophilic to clear cytoplasm, well defined borders and central elongated and occasionally wavy nuclei with evenly distributed chromatin and inconspicuous

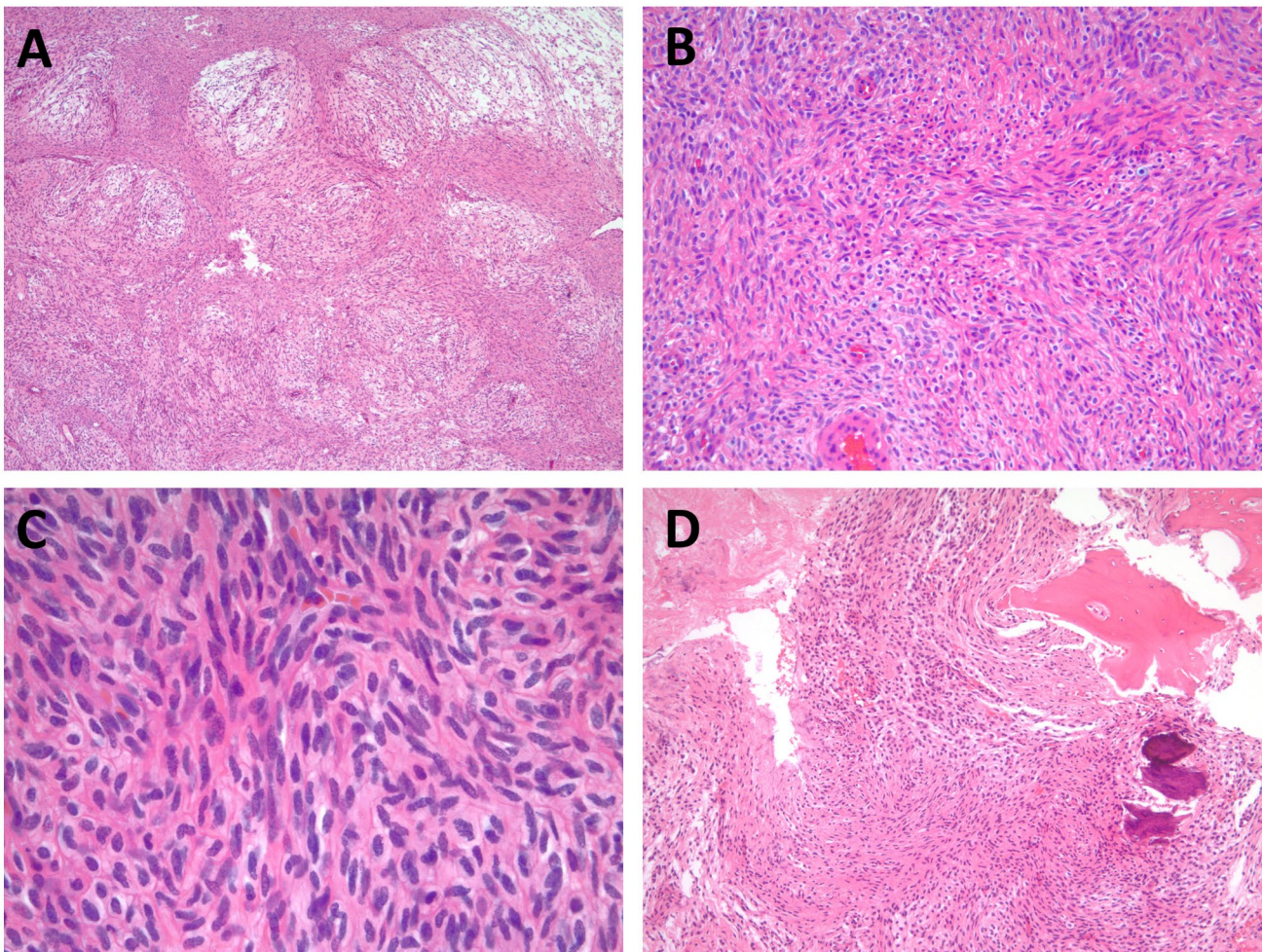


Fig. 2 Histologic features. **A** Histologic examination showed a spindle cell neoplasm with sharply demarcated areas of myxoid to collagenous background. **B & C** The more cellular areas showed the characteristic fascicular and herringbone arrangement of uniform plump cells with cleared cytoplasm, prominent borders and wavy to elongated euchromatic nuclei with no cytologic atypia. **D** Infiltrative growth was evident microscopically with entrapment of submucosal glands (not shown) and pre-existing bony trabeculae

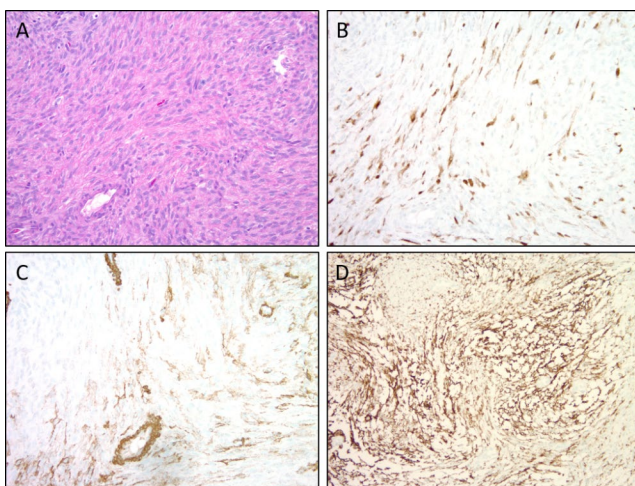


Fig. 3 Immunohistochemical stains. **A** typical cellular area of the tumor on a hematoxylin and eosin stained section (**A**). Neoplastic cells were focally positive for S100 (**B**) and smooth muscle actin (**C**). Pan-TRK showed increased cytoplasmic expression (**D**)

nucleoli. The cells appeared monotonous and showed no significant cytologic atypia or pleomorphism. Mitotic figures were extremely rare (< 1/10 HPF) and no tumor necrosis was seen. Scattered, compressed, thin-walled branching vessels and mast cells were seen throughout. Notably, hyperplastic surface epithelium was not appreciated and there was no evidence of rhabdomyoblastic differentiation.

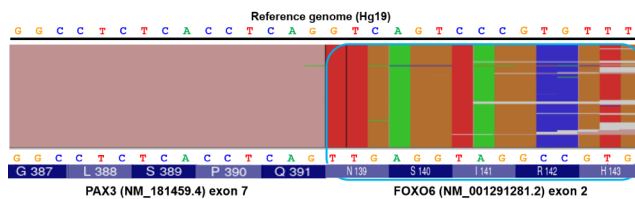
By immunohistochemistry (Fig. 3), the cells were focally positive for S100 and smooth muscle actin in the more cellular areas. The tumor was negative for keratins AE1/3 and CAM5.2, desmin, myogenin, CD34, SOX10, and STAT6. Beta-catenin demonstrated membranous reactivity but lacked nuclear expression. Interestingly, a pan-TRK immunostain showed increased cytoplasmic reactivity in tumor cells. See Table 1 for antibody details.

A diagnosis of BSS was favored based on the morphology and immunophenotypic features but due to the somewhat unusual pattern of cellularity, a next-generation

Table 1 Antibodies used for immunohistochemistry

Antibody	Clone	Source
S100	Polyclonal	Agilent
Smooth muscle actin	1A4	Cell Marque
SOX10	BC34	Biocare Medical
Beta-catenin	Clone 14	BD Bioscience
AE1/3	Cocktail	Cell Marque
Cam 5.2	Cocktail	BD Bioscience
Desmin	D33	Dako
Myogenin	F5D	Cell Marque
CD34	QBEnd/10	Cell Marque
STAT6	YE361	AbCam
Pan-TRK	EPR17341	AbCam

PAX3 exon 7 – FOXO6 exon 2 In-frame fusion



Fusion reads: 1676x (24.4%)

Fig. 4 NGS read alignment to the reference genome (Hg19) shows the identified *PAX3::FOXO6* fusion product. The *PAX3* exon 7 matched perfectly to the reference, while the *FOXO6* exon 2 (shown in the blue rectangle) mis-aligned to the *PAX3* intron 7 sequence. Noticed that the *PAX3* sequence is shown on the positive DNA strand

RNA-sequencing panel (NGS) was performed in order to confirm this impression. This recently developed NGS approach is capable of analyzing fragmented RNA transcripts extracted from formalin-fixed, paraffin-embedded tissues.[7] It uses nested polymerase chain reaction (PCR), with gene-specific and random PCR primers, to amplify cDNA of selected gene targets for sequencing. Since the reverse PCR primers were purposefully designed for random priming, this method is able to identify novel fusion gene partners that have not been reported previously. This RNA-based sequencing revealed abundant sequencing reads spanning the fusion juncture of a *PAX3::FOXO6* gene rearrangement. The fusion product is between *PAX3* exon 7 (NM_181459) and *FOXO6* exon 2 (NM_001291281.2) (Fig. 4). This fusion protein has not been reported in general fusion gene database (COSMIC, Mitelman, or Quiver) to the best of our knowledge. It is predicted to consist of the *PAX3* DNA binding domain and the *FOXO6* transcriptional activation domain. The fusion product is also predicted to

activate transcription from PAX-binding sites with higher potency than the corresponding wild-type PAX proteins.[8].

Six weeks after surgery, the patient reported improvement in symptoms. He was referred to radiation-oncology for further management. Given the low grade, tumor size, and negative margin status, the patient opted to undergo surveillance MRI every three months with the potential for salvage therapy if necessary. Signed patient consent was obtained for this report.

Discussion

Here, we describe the first reported case of BSS with a *PAX3::FOXO6* fusion protein. This is the first report of this fusion protein in BSS, and may be the first reported case of this fusion protein in any tumor. The majority (>50%–85%) of BSS demonstrate the t(2;4)(q35;q31.1) chromosomal rearrangement resulting in the fusion protein *PAX3::MAML3*, but other fusion partners have been described in smaller subsets of cases.[2, 5] *PAX3* rearrangements are seen in almost all cases (>90%) but alternative partner genes have included *FOXO1*, *NCOA1*, *NCOA2* and *WWTR1*. [2, 9–11] Larger studies examining the molecular findings in BSS demonstrate that up to 25% of BSS have *PAX3* rearrangements with partners other than those previously described.[1, 2] In each of these fusions, the 5' portion of *PAX3* to include exons 1–7 containing the DNA binding domains is expressed and paired with a transcriptional activator of the partner gene. Initial studies confirmed that the *PAX3::MAML3* fusion gene is a stronger transactivator of *PAX3* response elements than wild type *PAX3*. [5] Although the precise role of the partner gene in these fusions is not clear, there is strong evidence that *PAX3* activity is responsible for tumorigenesis. Clinical and prognostic implications of these various fusion proteins are not entirely clear due to the small numbers of cases, but data suggests that BSS with translocations other than *PAX3::MAML3* behave similarly to those that harbor *PAX3::MAML3* with slight variations in average patient age and tumor size.[2] Interestingly, similar, and in some cases, identical rearrangements (i.e. *PAX3::FOXO1* and *PAX3::NCOA2*) are also associated with alveolar rhabdomyosarcoma indicating that cell of origin and/or other factors play a role in tumor morphology and behavior even with the same molecular changes.[12–14].

PAX3 is located on the long arm of chromosome 2 and is part of the PAX transcription factor family. *PAX3* activity results in the downstream activation of multiple genes, including those involved in muscle, melanocytic, and neural development.[12, 15] In tumors with *PAX3* fusions, tumorigenesis is predicted to result from increased activation of

PAX3 response elements with detectable increases in a variety of genes including *NTRK3*. [5].

FOXO6, like *FOXO1*, is a member of the forkhead box gene transcription factor family (FOX proteins) and is located on the short arm of chromosome 1. [16] It is primarily expressed in the central nervous system and targets multiple cellular processes including apoptosis, cell signaling, and cellular differentiation. [16, 17] It has also been implicated in activating hepatic gluconeogenesis. [18] While other FOX proteins such as FOXO1 and FOXO3 play important roles in skeletal muscle homeostasis, the role of FOXO6 in skeletal muscle is less clear. However, recent studies have suggested that FOXO6 may play a role in skeletal muscle metabolism. [19, 20] Given the homology between FOX genes, we hypothesize that FOXO6 plays a similar role as FOXO1 in *PAX3::FOXO1* fusions.

The clinical presentation, along with the microscopic and immunophenotypic features of the current case were characteristic of BSS. The spindled cells had a low mitotic count and no necrosis. They expressed smooth muscle actin and S100, therefore demonstrating both a muscular and neural phenotype. [3, 21] Although BSS is known to occasionally demonstrate areas of rhabdomyoblastic differentiation, this was not seen in our case. Other entities on the differential diagnosis of a spindled sinonasal lesion, such as solitary fibrous tumor, synovial sarcoma, leiomyosarcoma, and spindle cell rhabdomyosarcoma, were effectively ruled out with immunohistochemistry and molecular studies.

Our case of BSS with a novel fusion protein has been predicted by past studies in which rare BSS cases had an unidentifiable *PAX3* fusion partner at the time of the study. [2, 9] Interestingly, *PAX3::FOXO6* has not been reported in any diagnostic entity to our knowledge. As *PAX3* plays an important role in skeletal muscle and neural development and *FOXO6* is important in neural development (and possibly skeletal muscle homeostasis), the presence of a fusion protein between those two entities supports the diagnosis of BSS given the morphology and staining characteristic in our opinion. Given that BSS is a rare and relatively recently characterized tumor, it is possible that further molecular analysis may identify additional novel fusions with possible clinical and diagnostic implications.

Funding None.

Data Availability Available on request.

Code Availability Not applicable.

Declarations

Conflict of Interest The authors have no conflicts of interest.

Ethics Approval Not applicable per Cleveland Clinic IRB (case report with patient consent).

Consent to Participate The patient has signed a consent for this case report.

Consent for Publication The patient has signed a consent for this case report.

References

- Andreasen S, Bishop JA, Hellquist H, Hunt J, Kiss K, Rinaldo A, et al. Biphenotypic sinonasal sarcoma: demographics, clinicopathological characteristics, molecular features, and prognosis of a recently described entity. *Virchows Arch* [Internet]. *Virchows Arch*; 2018 [cited 2022 May 19];473:615–26. Available from: <https://pubmed.ncbi.nlm.nih.gov/30109475/>.
- Fritchie KJ, Jin L, Wang X, Graham RP, Torbenson MS, Lewis JE, et al. Fusion gene profile of biphenotypic sinonasal sarcoma: an analysis of 44 cases. *Histopathology* [Internet]. *Histopathology*; 2016 [cited 2022 May 19];69:930–6. Available from: <https://pubmed.ncbi.nlm.nih.gov/27454570/>.
- Lewis JT, Oliveira AM, Nascimento AG, Schembri-Wismayer D, Moore EA, Olsen KD, et al. Low-grade sinonasal sarcoma with neural and myogenic features: a clinicopathologic analysis of 28 cases. *Am J Surg Pathol* [Internet]. *Am J Surg Pathol*; 2012 [cited 2022 May 19];36:517–25. Available from: <https://pubmed.ncbi.nlm.nih.gov/22301502/>.
- Rooper LM, Huang SC, Antonescu CR, Westra WH, Bishop JA. Biphenotypic sinonasal sarcoma: an expanded immunoprofile including consistent nuclear β -catenin positivity and absence of SOX10 expression. *Hum Pathol* [Internet]. *Hum Pathol*; 2016 [cited 2022 May 19];55:44–50. Available from: <https://pubmed.ncbi.nlm.nih.gov/27137987/>.
- Wang X, Bledsoe KL, Graham RP, Asmann YW, Viswanatha DS, Lewis JE, et al. Recurrent PAX3-MAML3 fusion in biphenotypic sinonasal sarcoma. *Nat Genet* [Internet]. *Nat Genet*; 2014 [cited 2022 May 19];46:666–8. Available from: <https://pubmed.ncbi.nlm.nih.gov/24859338/>.
- Jo VY, Mariño-Enríquez A, Fletcher CDM, Hornick JL. Expression of PAX3 Distinguishes Biphenotypic Sinonasal Sarcoma From Histologic Mimics. *Am J Surg Pathol* [Internet]. *Am J Surg Pathol*; 2018 [cited 2022 Jun 1];42:1275–85. Available from: <https://pubmed.ncbi.nlm.nih.gov/29863547/>.
- Cheng YW, Meyer A, Jakubowski MA, Keenan SO, Brock JE, Azzato EM, et al. Gene Fusion Identification Using Anchor-Based Multiplex PCR and Next-Generation Sequencing. *J Appl Lab Med* [Internet]. *J Appl Lab Med*; 2021 [cited 2022 Jun 20];6:917–30. Available from: <https://pubmed.ncbi.nlm.nih.gov/33537766/>.
- Barr FG. Gene fusions involving PAX and FOX family members in alveolar rhabdomyosarcoma. *Oncogene* [Internet]. *Oncogene*; 2001 [cited 2022 May 19];20:5736–46. Available from: <https://pubmed.ncbi.nlm.nih.gov/11607823/>.
- Huang SC, Ghossein RA, Bishop JA, Zhang L, Chen TC, Huang HY, et al. Novel PAX3-NCOA1 Fusions in Biphenotypic Sinonasal Sarcoma With Focal Rhabdomyoblastic Differentiation. *Am J Surg Pathol* [Internet]. *Am J Surg Pathol*; 2016 [cited 2022 May 19];40:51–9. Available from: <https://pubmed.ncbi.nlm.nih.gov/26371783/>.
- Wong WJ, Lauria A, Hornick JL, Xiao S, Fletcher JA, Marino-Enriquez A. Alternate PAX3-FOXO1 oncogenic fusion in biphenotypic sinonasal sarcoma. *Genes Chromosomes Cancer*

- [Internet]. *Genes Chromosomes Cancer*; 2016 [cited 2022 Jun 1];55:25–9. Available from: <https://pubmed.ncbi.nlm.nih.gov/26355893/>.
11. Loarer F, Le, Laffont S, Lesluyes T, Tirode F, Antonescu C, Baglin AC, et al. Clinicopathologic and Molecular Features of a Series of 41 Biphenotypic Sinonasal Sarcomas Expanding Their Molecular Spectrum. *Am J Surg Pathol* [Internet]. *Am J Surg Pathol*; 2019 [cited 2022 Jun 2];43:747–54. Available from: <https://pubmed.ncbi.nlm.nih.gov/30829729/>.
 12. Boudjadi S, Chatterjee B, Sun W, Vemu P, Barr FG. The expression and function of PAX3 in development and disease. *Gene* [Internet]. *Gene*; 2018 [cited 2022 May 19];666:145–57. Available from: <https://pubmed.ncbi.nlm.nih.gov/29730428/>.
 13. Leiner J, Le Loarer F. The current landscape of rhabdomyosarcomas: an update. *Virchows Arch* [Internet]. *Virchows Arch*; 2020 [cited 2022 May 19];476:97–108. Available from: <https://pubmed.ncbi.nlm.nih.gov/31696361/>.
 14. Sumegi J, Streblov R, Frayer RW, Cin PD, Rosenberg A, Meloni-Ehrig A, et al. Recurrent t(2;2) and t(2;8) translocations in rhabdomyosarcoma without the canonical PAX-FOXO1 fuse PAX3 to members of the nuclear receptor transcriptional coactivator family. *Genes Chromosomes Cancer* [Internet]. *Genes Chromosomes Cancer*; 2010 [cited 2022 Jun 2];49:224–36. Available from: <https://pubmed.ncbi.nlm.nih.gov/19953635/>.
 15. Buckingham M, Relaix F. PAX3 and PAX7 as upstream regulators of myogenesis. *Semin Cell Dev Biol* [Internet]. *Semin Cell Dev Biol*; 2015 [cited 2022 May 19];44:115–25. Available from: <https://pubmed.ncbi.nlm.nih.gov/26424495/>.
 16. Jacobs FMJ, Van der Heide LP, Wijchers PJEC, Burbach JPH, Hoekman MFM, Smidt MP. FoxO6, a novel member of the FoxO class of transcription factors with distinct shuttling dynamics. *J Biol Chem* [Internet]. *J Biol Chem*; 2003 [cited 2022 May 19];278:35959–67. Available from: <https://pubmed.ncbi.nlm.nih.gov/12857750/>.
 17. Link W. Introduction to FOXO Biology. *Methods Mol Biol* [Internet]. *Methods Mol Biol*; 2019 [cited 2022 May 19];1890:1–9. Available from: <https://pubmed.ncbi.nlm.nih.gov/30414140/>.
 18. Kim DH, Perdomo G, Zhang T, Slusher S, Lee S, Phillips BE, et al. FoxO6 integrates insulin signaling with gluconeogenesis in the liver. *Diabetes* [Internet]. *Diabetes*; 2011 [cited 2022 May 19];60:2763–74. Available from: <https://pubmed.ncbi.nlm.nih.gov/21940782/>.
 19. Sanchez AMJ, Candau RB, Bernardi H. FoxO transcription factors: their roles in the maintenance of skeletal muscle homeostasis. *Cell Mol Life Sci* [Internet]. *Cell Mol Life Sci*; 2014 [cited 2022 May 19];71:1657–71. Available from: <https://pubmed.ncbi.nlm.nih.gov/24232446/>.
 20. ZHANG L, ZHANG Y, ZHOU M, WANG S, LI T, HU Z, et al. Role and mechanism underlying FoxO6 in skeletal muscle in vitro and in vivo. *Int J Mol Med* [Internet]. *Int J Mol Med*; 2021 [cited 2022 May 19];48. Available from: <https://pubmed.ncbi.nlm.nih.gov/34080654/>.
 21. Thompson LDR, Franchi A. New tumor entities in the 4th edition of the World Health Organization classification of head and neck tumors: Nasal cavity, paranasal sinuses and skull base. *Virchows Arch* [Internet]. *Virchows Arch*; 2018 [cited 2022 May 19];472:315–30. Available from: <https://pubmed.ncbi.nlm.nih.gov/28444451/>.

Publisher's Note Springer Nature remains neutral with regard to jurisdictional claims in published maps and institutional affiliations.

Springer Nature or its licensor holds exclusive rights to this article under a publishing agreement with the author(s) or other rightsholder(s); author self-archiving of the accepted manuscript version of this article is solely governed by the terms of such publishing agreement and applicable law.